J. Min. Metall. Sect. B-Metall. 55 (3) B (2019) 405 - 411

Journal of Mining and Metallurgy, Section B: Metallurgy

SPHEROIDIZATION HEAT TREATMENT AND INTERCRITICAL ANNEALING OF LOW CARBON STEEL

Z. Nasiri and H. Mirzadeh*

* School of Metallurgy and Materials Engineering, College of Engineering, University of Tehran, Tehran, Iran

(Received 13 August 2018; accepted 16 May 2019)

Abstract

Spheroidization annealing of low carbon steel and its effects on the microstructure and mechanical properties of dual phase (DP) steel were studied. It was revealed that the reduction in strength and hardness of the quenched martensitic microstructure was much more pronounced compared to the fully annealed ferritic-pearlitic banded microstructure with spheroidizing time. This was related to the confinement of spheroidized carbide particles to distinct bands in the latter, and the uniform dispersion of carbides and high-temperature tempering of martensite in the former. During intercritical annealing of the spheroidized microstructures, the tendency to obtain martensite particles as discrete islands was observed. This, in turn, resulted in an inferior strength-ductility balance compared to the DP steel obtained from the intercritical annealing of martensite, which negated the usefulness of the spheroidized microstructures as the initial microstructures for the processing of DP steels.

Keywords: *DP steels; Spheroidizing treatment; Microstructure; Mechanical properties; Strain hardening rate*

1. Introduction

Normally, the low-carbon dual phase (DP) steels have a duplex ferritic-martensitic microstructure, which is responsible for the observed high strength-ductility balance and continuous yielding [1-3]. Their tensile properties are largely determined by the volume fraction and the morphology of martensite [4]. The morphology can be controlled by changing the initial microstructure using heat treatment [5-11] and thermomechanical processing routes [12-17].

One of the processing routes to alter the initial microstructure is the spheroidization treatment. The reduction of interfacial energy associated with carbide interfaces provides a powerful thermodynamic driving force for microstructural changes in steel, and hence, the spheroidized microstructures are the most stable that can be produced [18,19]. Spheroidizing is more rapid than in pearlitic microstructures if the particles are formed by the tempering of martensite [20-22]. Many other approaches to spheroidizing are used to accelerate the process: heating to accomplish either complete or partial austenitizing and then holding just below A_{C1}, cooling quickly through the A_{C1}, or cycling above and below A_{C1} [23-28].

The fully spheroidized microstructure is considered as one of the initial ones for the intercritical annealing to produce DP steels [9,29]. In commercial practice, widely spaced and coarse carbides are required to reduce hardness and increase ductility. However, microstructures corresponding to the intermediate stages of the spheroidization heat treatment can be also used as the initial microstructures for the intercritical annealing to change the attributes of microstructural features. Studies dealing with spheroidizing revealed that during this treatment, significant microstructural changes happen [18-28]. For DP steels, the microstructural modification effects of the spheroidization treatment have not been studied to date and the present work aims to deal with this subject. In this regard, the banded ferritic-pearlitic and martensitic microstructures were considered for spheroidization annealing and subsequent intercritical heat treatment of a low carbon steel.

2. Experimental details

A fully annealed 0.18C-0.14Si-1.29Mn-0.022Cu-0.083Ni-0.017P-0.004S steel sheet was used. Based on the Trzaska and Park equations [30,31], the A_1 and A_3 temperatures were estimated as ~726 and ~865 °C,

*Corresponding author: hmirzadeh@ut.ac.ir

https://doi.org/10.2298/JMMB180813033N

respectively. As shown in Fig. 1, the as-received sheet was austenitized at 1050 °C followed by water quenching to obtain the martensitic microstructure. Afterwards, the initial fully annealed and quenched microstructures were considered as the starting ones for investigating the spheroidization heat treatment at 700 ºC for 1, 3, 9, and 24 h. The holding time at 700 ºC was termed as "spheroidization time" for the sake of brevity. Finally, all these steels were intercritically annealed at 735 ºC for 15 minutes and then water quenched to produce dual phase microstructures with martensite volume fraction of ~0.3.

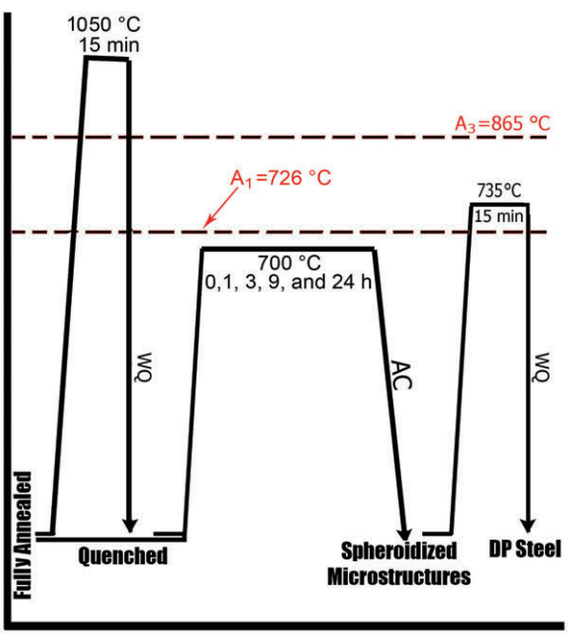

Figure 1. *Schematic representation of the processing routes employed in this study. AC and WQ represent air cooling and water quenching, respectively*

The 2% Nital solution was used to reveal the microstructures. The microstructural investigations were performed using an Olympus Vanox optical microscope and a Vega Tescan scanning electron microscope (SEM) equipped with energy-dispersive spectroscopy (EDS). The tensile specimen was prepared according to JIS-Z-2201 standard [32] with a gage length of 12 mm and the crosshead speed of the tensile test was 1 mm/min. These tests were repeated once to ensure the reproducibility of the results. For calculating the incremental work-hardening exponents (n), the Hollomon equation [33] was expressed as $\ln\sigma = \ln k + n\ln\varepsilon$, and at a given strain, the slope of the plot of lnσ versus lnε was determined. Simply, it can be express as $n = d\ln\sigma / d\ln\varepsilon$. For obtaining the slope, the central difference approach [34-37] based on $n\big|_i = \{\ln\sigma_{i+1} - \ln\sigma_{i-1}\} / \{\ln\varepsilon_{i+1} - \ln\varepsilon_{i-1}\}$ was utilized. Hardness measurements were performed using a Vickers hardness tester under a load of 20 kg. Finally, phase identification was performed by x-ray diffraction (XRD) technique using a PHILIPS diffractometer with Cu-kα radiation.

3. Results and discussion

3.1 Spheroidization heat treatment

Fig. 2 shows the evolution of starting microstructures during spheroidization treatment at 700 ºC along with the variation of hardness. The fully annealed sample (denoted as 0 h) had a well-defined banded microstructure, as expected [38]. During spheroidization treatment, the spheroidized carbides started to appear in the pearlite bands, and after 24 h, they were easily identified. The hardness measurements revealed that this treatment slightly reduced the hardness and did not have a major effect on the hardness. This can be explained based on the confinement of the carbides to some distinct bands.

The SEM image of the quenched microstructure (denoted as 0 h) is also shown in Fig. 2 and exhibits a typical lath martensite morphology. During spheroidization, which is essentially a high-temperature tempering treatment [39,40], the spheroidized carbide particles started to appear in the martensitic microstructure and a uniform distribution of spheroidized carbides in the tempered microstructure was seen by continued tempering. The change of hardness in this case was quite noticeable. After just 1 h at 700 ºC, the hardness dropped from 507 ± 26 HV to 207 ± 6 HV, and after 24 h, it dropped to 180 ± 8 HV. This rapid fall was related to the tempering of martensite, during which the recovery processes and decreasing tetragonality due to carbon loss are dominant [39,40].

The EDX spot analyses taken from the matrix and some particles of the quenched sample after

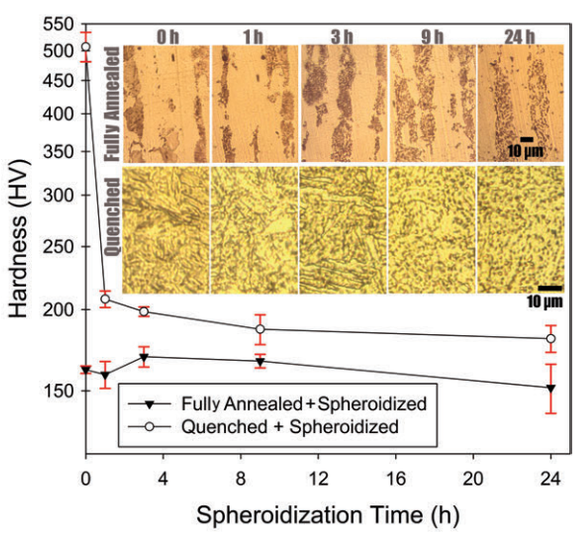

Figure 2. *Microstructural evolution and hardness measurements during spheroidization treatment*

spheroidization time of 24 h are shown in Fig. 3a, and they revealed that the matrix was mainly composed of iron, while the particles had high amount of C, indicating the presence of spheroidized carbide particles. The XRD pattern taken from this sample is shown in Fig. 3b, and exhibited diffraction peaks of ferrite. However, the diffraction peaks of the carbide phase were not revealed, due to the small amount of this phase.

Comparing the hardness of spheroidized microstructures after 24 h with fully annealed and quenched initial microstructures revealed that the hardness of the latter was higher than the former. This might be explained by the fact that, for the quenched sample as the initial microstructure, the carbide particles were uniformly distributed and the matrix is tempered martensite [39], which provided more effective barrier to dislocation motion.

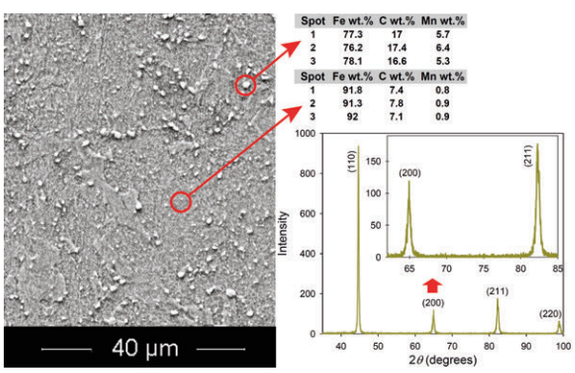

Figure 3. *EDX spot analyses taken from the matrix and particles, with the XRD pattern for the quenched sample after spheroidization time of 24 h*

The tensile curves of the studied materials are shown in Fig. 4 and the tensile data are summarized in Table 1, where the overall strength of the samples was in general agreement with the observed trends in hardness measurements. Moreover, by increasing strength, the total elongation declined as expected. Furthermore, the fully annealed and also both samples that were spheroidized for 24 h showed a well-defined yield point, which is related to the Cottrell atmospheres produced by interstitial atoms around dislocations [41].

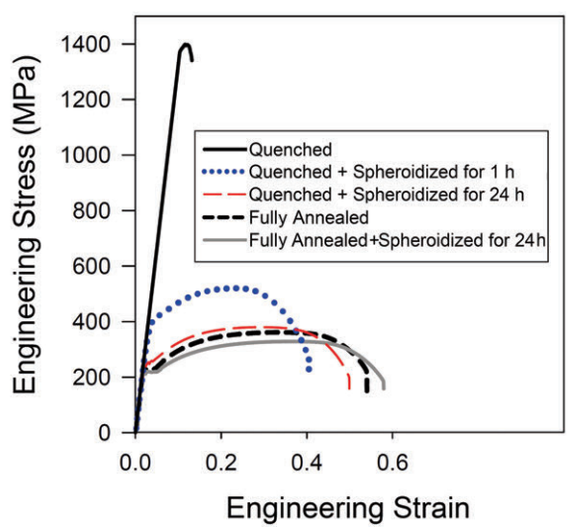

Figure 4. *Tensile stress-strain curves before intercritical heat treatment*

Table 1. *Summary of tensile data*

Sample	Yield Stress (MPa)	Tensile Strength (MPa)	Total Elongation (%)
Quenched	1377 ± 7	1405 ± 6	3 ± 1
Quenched + Spheroidized for 1 h	381 ± 3	520 ± 4	37 ± 2
Quenched + Spheroidized for 24 h	224 ± 4	380 ± 3	48 ± 2
Fully Annealed	208 ± 2	361 ± 4	52 ± 1
Fully Annealed + Spheroidized for 24 h	206 ± 6	328 ± 4	58 ± 2

3.2 Intercritical annealing

Fig. 5 shows the microstructural and hardness evolutions after spheroidization treatment at 700 °C followed by intercritical annealing at 735 °C for 15 min and water quenching. The DP microstructure obtained from the fully annealed sample had a martensitic-ferritic banded microstructure, inherited from the initial pearlitic-ferritic banded microstructure. The martensite particles were seen for the samples corresponding to spheroidization times of 1, 3, 9, and 24 h. After 24 h, the microstructure resembles a banded one with martensite particles inside bands. The hardness measurements revealed that the hardness values of these DP steels (Fig. 5) were higher than their initial spheroidization annealed counterparts (Fig. 2). This is related to the replacement of ferrite/pearlite microstructures with ferrite/martensite ones. Higher hardness of martensite resulted in the higher hardness of the intercritically annealed samples. Moreover, based on the image analysis of the fully annealed sample (Fig. 2), the volume percent of pearlite was obtained as ~21%. The volume percent of martensite in the corresponding intercritically annealed sample was determined as ~30% (Fig. 5). The higher volume fraction of ~30% provided evidence that the second phase particles in Fig. 5 were not pearlite (or carbides).

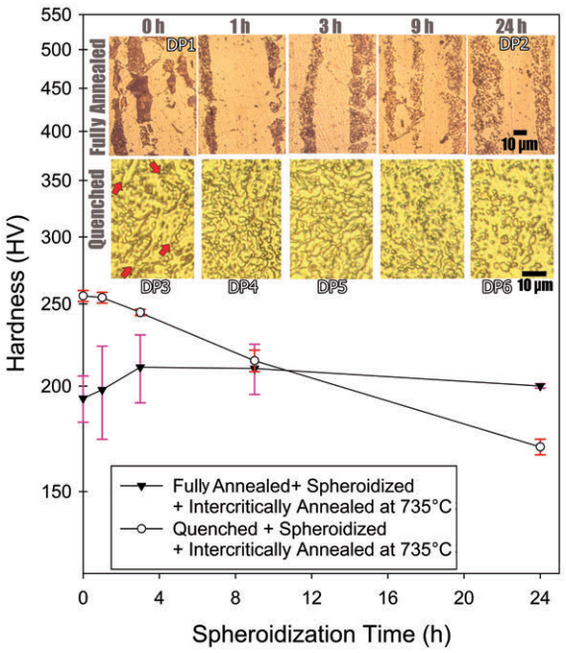

Figure 5. *Microstructural evolution and hardness measurements after intercritical heat treatment of spheroidized samples*

The DP microstructure obtained from the quenched sample is also shown in Fig. 5, where the original lath martensitic morphology was easily discerned due to the formation of austenite (martensite after quenching) on the boundaries provided by the martensitic microstructure (some of them are shown by arrows), which was consistent with the previous research works [42-45]. The other DP microstructures were related to their initial spheroidization annealed counterparts (Fig. 2). After 24 h, a microstructure with uniformly dispersed martensite particles was identified. For this sample, the corresponding EDX spot analyses taken from the matrix and martensite particles are shown in Fig. 6a, which revealed that both matrix and particles had carbon contents similar to that of matrix in Fig. 3a. Therefore, the particles were not characterized as carbide. Moreover, the volume fraction of particles was around the expected martensite volume fraction of 30%. Therefore, these particles were considered as martensite islands. The formation of austenite in place of spheroidized carbides during intercritical annealing has been also noted in the literature. For instance, Bag et al. [42] and other researchers [43-45] showed that the nucleation of austenite from the tempered martensite can occur at different sites, such as the prior austenite grain boundaries, the carbide precipitates on prior austenite grain boundaries, the spheroids in ferrite, and the fine carbide arrays formed on the prior martensitic plate/lath boundaries. The XRD pattern taken from this sample is also shown in Fig. 6b, which only revealed the presence of ferritic-type phases (ferrite and martensite). The original evidence for martensite lattice tetragonality came from the splitting of (002) and (200) peaks on X-ray diffractograms [46,47]. The magnification of (200) and (211) peaks is shown in Fig. 6c, where the diffraction doublets were not clearly resolved. It has been reported that for steels with less than 0.6 wt.% C, the peak split cannot be identified [46]. However, compared to Fig. 3c, the broadening and decreased intensity of this peak were obvious, which indicated the change in the diffraction pattern.

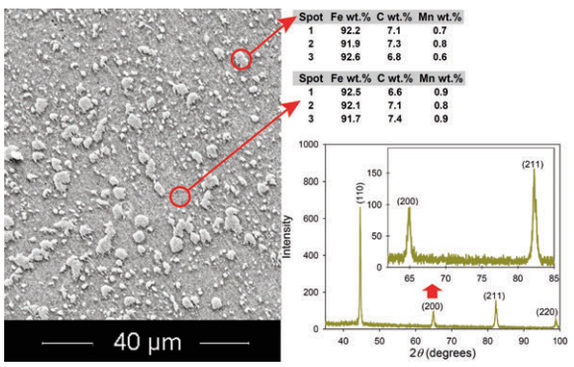

Figure 6. *EDX spot analyses taken from the matrix and particles with the XRD pattern for the quenched sample after spheroidization time of 24 h and intercritical annealing (DP 6)*

The hardness measurements (Fig. 5) revealed that the hardness did not change considerably up to 1 h, but afterwards when the martensite particles appeared in the microstructure, it rapidly decreased. After 24 h, the hardness of the DP steel with the quenched initial microstructure was below that of the fully annealed counterpart (Fig. 5). The opposite trend was observed in Fig. 2 for the spheroidized samples before intercritical annealing. In other words, after 24 h, the spheroidized banded microstructure had lower hardness compared to the microstructure with dispersed spheroidized carbides, but the martensite particles in the bands resulted in higher hardness compared to the microstructure with the dispersion of the martensite particles. Therefore, these findings can be explained based on the presence of martensite in the microstructure, as will be treated in the following by consideration of tensile properties.

The tensile curves are shown in Fig. 7. The absence of the yield point was evident. It is well-known [1,48] that the unlocked dislocations induced by the austenite-to-martensite transformation during quenching are responsible for this.

Figure 7 shows that the intercritically annealed sample in the quenched state (DP3) had the highest tensile strength among DP steels. In the previous studies [7-10], the initial martensitic microstructure was found to be one of the appropriate ones for

obtaining DP steel by intercritical annealing. Here, it was seen that it had better strength and ductility compared to the intercritically annealed sample originating from the fully annealed sample (DP1). By spheroidization annealing, the tensile strength decreased for the tensile curves of DP2, DP4 and DP6 steels (Fig. 7). This was ascribed to the fact that the martensite phase tends to become discrete islands as a result of increasing spheroidization time before intercritical annealing. Thus, its reinforcing effects diminish [41]. Another observation to support this finding can be realized by comparing DP2 with DP 6. The martensite particles in the bands (DP2, the microstructure after 24 h spheroidizing in Fig. 5) resulted in a higher strength compared to the dispersed martensite particles in the microstructure (DP6). The similar trend was also found for hardness, as described above.

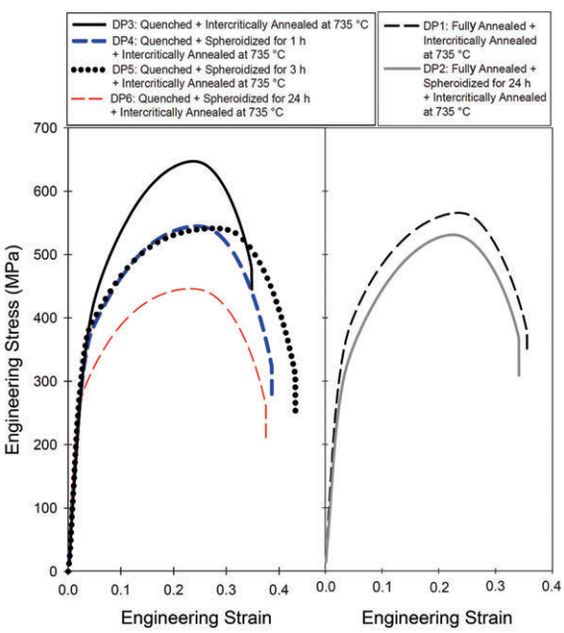

Figure 7. *Tensile stress-strain curves after intercritical heat treatment*

A comparison between incremental work-hardening exponents is shown in Fig. 8, which reveals that the *n*-values of DP3 were higher than others. Therefore, it can be deduced that the work-hardening capacity of DP3 steel was the best. Figure 8 also shows the summary of the tensile properties in the form of a strength-ductility balance. The DP steels are located above the curve of strength-ductility balance drawn for the steels with conventional microstructures in this work. By increasing spheroidization time, the tensile strength decreased but the elongation increased up to the spheroidization time of 3 h. Afterwards, the strength-ductility balance of the spheroidization time of 24 h was below the curve. Similarly, the point corresponding to the spheroidized DP steel (DP2) with banded morphology also was below this curve. This meant that the tensile properties of completely spheroidized samples were inferior compared to the usual trend observed in these data. The usual trend was obtained by consideration of samples that were not intercritically annealed. Based on these results, it was deduced that the time-consuming and expensive spheroidization treatment is not a viable method for processing of low-carbon DP steels.

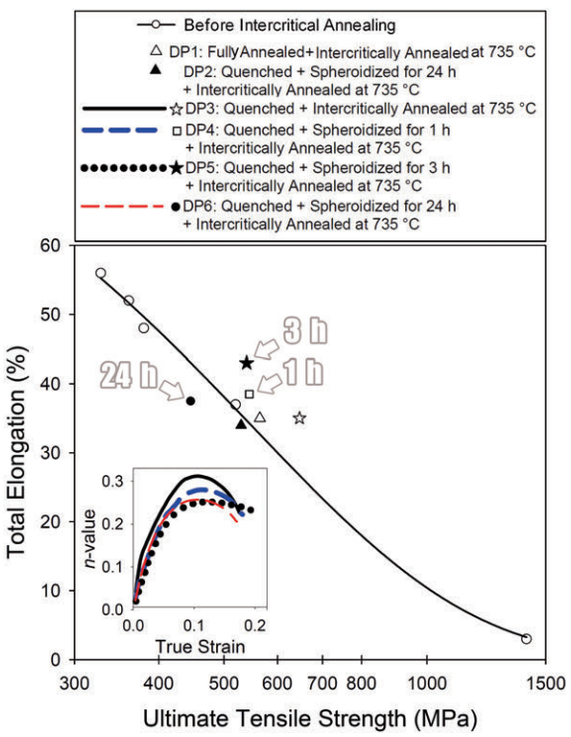

Figure 8. *Summary of tensile properties*

4. Conclusions

This work studied the spheroidization annealing of low carbon steel and its effects on the resultant dual phase steels. The following conclusions were drawn:

(1) During spheroidization treatment, the change in hardness and tensile strength revealed that this treatment slightly reduced the hardness and strength of the ferritic-pearlitic banded microstructure, due to the fact that the carbide phase had been confined to some distinct bands. However, during the spheroidization treatment of martensitic microstructure, which is essentially a high-temperature tempering treatment, the change in hardness and tensile strength was notable due to the dominancy of recovery processes and carbon loss to form carbides.

(2) After intercritical annealing, the hardnesses of the DP steels were higher than their initial

spheroidization annealed counterparts. After long-term spheroidization of the fully annealed microstructure, martensite particles appeared in the prior pearlite bands. However, for the quenched sample, a microstructure with uniformly dispersed martensite particles was obtained.

(3) Higher strength and ductility was obtained after intercritical annealing of the martensitic microstructure compared to the initial fully annealed one. By spheroidizing, the tensile strength decreased as a result of the tendency of martensite phase to form discrete islands. After intercritical annealing, the strength and hardness of the long-term spheroidized sample from the initial martensitic microstructure was below that of the ferritic-pearlitic microstructure, which supported this finding.

(4) The tensile properties were summarized and the properties of DP steels were above the conventional curve of strength-ductility balance. By increasing spheroidization time, the tensile strength decreased but the elongation increased after short annealing times. For longer spheroidization time, the strength-ductility balance corresponding to the DP steel was below the curve, showing that the tensile properties of samples with spheroidized particles were inferior compared to the usual trend observed in data.

Acknowledgments

The authors would like to greatly thank the members of the Advanced Steels and Thermomechanically Processed Engineering Materials Laboratory for their help and support. Financial support by the University of Tehran is also gratefully acknowledged.

References

[1] S. Nikkhah, H. Mirzadeh, M. Zamani, Mater. Chem. Phys., 230 (2019) 1-8.

[2] C.C. Tasan, M. Diehl, D. Yan, M. Bechtold, F. Roters, L. Schemmann, C. Zheng, N. Peranio, D. Ponge, M. Koyama, K. Tsuzaki, D. Raabe, Annu. Rev. Mater. Res., 45 (2015) 19.1-19.41.

[3] S. Nikkhah, H. Mirzadeh, M. Zamani, Mater. Sci. Eng. A, 756 (2019) 268-271.

[4] Y. Tomita, J. Mater. Sci., 25 (1990) 5179-5184.

[5] H. Seyedrezai, A.K. Pilkey, J.D. Boyd, Mater. Sci. Eng. A, 594 (2014) 178-188.

[6] S. Ghaemifar, H. Mirzadeh, Steel Re. Int., 89 (2018) 1700531.

[7] D. Das, P.P. Chattopadhyay, J. Mater. Sci., 44 (2009) 2957-2965.

[8] F. Jamei, H. Mirzadeh, M. Zamani, Mater. Sci. Eng. A, 750 (2019) 125-131.

[9] X.L. Cai, A.J. Garratt-Reed, W.S. Owen, Metall. Trans. A 16 (1985) 543-557.

[10] N. Shukla, S. Das, S. Maji, S.R. Chowdhury, B.K. Show, J. Mater. Eng. Perform., 24 (2015) 4958-4965.

[11] H. Ashrafi, S. Sadeghzade, R. Emadi, M. Shamanian, Steel Re. Int., 88 (2017) 1600213.

[12] M. Nouroozi, H. Mirzadeh, M. Zamani, Mater. Sci. Eng. A, 736 (2018) 22-26.

[13] M. Papa Rao, V. Subramanya Sarma, S. Sankaran, Metall. Mater. Trans. A, 45 (2014) 5313-5317.

[14] A. Karmakar, M. Mandal, A. Mandal, Md. Basiruddin Sk, S. Mukherjee, D. Chakrabarti, Metall. Mater. Trans. A, 47 (2016) 268-281.

[15] M. Zamani, H. Mirzadeh, M. Maleki, Mater. Sci. Eng. A, 734 (2018) 178-183.

[16] H. Azizi-Alizamini, M. Militzer, W.J. Poole, ISIJ Int., 51 (2011) 958-964.

[17] H. Mirzadeh, M. Alibeyki, M. Najafi, Metall. Mater. Trans. A, 48 (2017) 4565- 4573.

[18] G. Krauss, Steels Processing, Structure, and Performance, 2nd edition, Russell Township, ASM International 2015.

[19] Z. Nasiri, H. Mirzadeh, Materwiss. Werksttech., 49 (2018) 108-1086.

[20] E. Karadeniz, Mater. Des., 29 (2008) 251-256.

[21] Y.W. Lee, Y. Son, S.J. Lee, Mater. Sci. Eng. A, 585 (2013) 94-99.

[22] Z.Q. Lv, B. Wang, Z.H. Wang, S.H. Sun, W.T. Fu, Mater. Sci. Eng. A, 574 (2013) 143-148.

[23] D. Hernández-Silva, R.D. Morales, J.G. Cabañas-Moreno, ISIJ Int., 32 (1992) 1297-1305.

[24] J.M. O'Brien, W.F. Hosford, Metall. Mater. Trans. A, 33 (2002) 1255-1261.

[25] A. Saha, D.K. Mondal, J. Maity, Mater. Sci. Eng. A, 527 (2010) 4001-4007.

[26] A. Karnyabi-Gol, M. Sheikh-Amid, J. Iron Steel Res. Int., 17 (2010) 45-52.

[27] L.W. Ma, K. Xia, Kovove Mater., 49 (2011) 23-27.

[28] K.M. Vedula, R.W. Heckel, Metall. Trans. 1 (1970) 9-18.

[29] A. Kalhor, H. Mirzadeh, Steel Res. Int., 88 (2017) 1600385.

[30] M. Maleki, H. Mirzadeh, M. Zamani, J. Mater. Eng. Perform., 28 (2019) 2178-2183.

[31] S. Ghaemifar, H. Mirzadeh, Can. Metall. Q., 56 (2017) 459-463.

[32] JIS Z 2201, Test pieces for tensile test for metallic materials, Japanese Standards Association 1988.

[33] G.E. Dieter, Mechanical Metallurgy, third ed., McGraw-Hill 1988.

[34] S. Saadatkia, H. Mirzadeh, J.M. Cabrera, Mater. Sci. Eng. A, 636 (2015) 196-202.

[35] F. Najafkhani, H. Mirzadeh, M. Zamani, Met. Mater. Int., 25 (2019) 1039-1046.

[36] H. Mirzadeh, J.M. Cabrera, J.M. Prado, A. Najafizadeh, Mater. Sci. Eng. A, 528 (2011) 3876-3882.

[37] B. Pourbahari, H. Mirzadeh, M. Emamy, R. Roumina, Adv. Eng. Mater., 20 (2018) 1701171.

[38] M. Maleki, H. Mirzadeh, M. Zamani, Steel Res. Int., 89 (2018) 1700412.

[39] G. Krauss, Steel Res. Int., 88 (2017) 1700038.

[40] M. Najafi, H. Mirzadeh, M. Alibeyki, J. Min. Metall.

Sect. B-Metall., 55 (2019) 95-99.
[41] J. Rösler, H. Harders, M. Bäker, Mechanical behavior of engineering materials, Springer, Berlin 2007.
[42] A. Bag, K.K. Ray, E.S. Dwarakadasa, Metall. Mater. Trans. A, 30 (1999) 1193-1202.
[43] G.R. Speich, V.A. Demarest, R.L. Miller, Metall. Mater. Trans. A, 12 (1981) 1419-1428.
[44] M. Mazinani, Deformation and fracture behaviour of a low-carbon dual-phase steel, Ph.D. Thesis, University of British Columbia 2006.
[45] J. Huang, W.J. Poole, M. Militzer, Metall. Mater. Trans. A, 35 (2004) 3363-3375.
[46] V.A. Lobodyuk, Y.Y. Meshkov, E.V. Pereloma, Metall. Mater. Trans. A, 50 (2019) 97-103.
[47] T. Waterschoot, K. Verbeken, ISIJ Int., 46 (2006) 138-146.
[48] C. Thomser, V. Uthaisangsuk, W. Bleck, Steel Res. Int., 80 (2009) 582- 587.

TERMIČKA OBRADA SFEROIDIZACIJOM I MEĐUKRITIČNO ŽARENJE ČELIKA SA NISKIM SADRŽAJEM UGLJENIKA

Z. Nasiri and H. Mirzadeh*

* Fakultet za metalurgiju i inženjerstvo materijala, Univerzitet u Teheranu, Teheran, Iran

Apstrakt

Proučavano je sferično žarenje niskougljeničnog čelika i efekti tog postupka na mikrostrukturu i mehaničke osobine dvofaznog (DP) čelika. Pokazalo se da je smanjenje snage i tvrdoće kaljene martenzitne strukture mnogo izraženije u poređenju sa potpuno žarenom feritno-perlitnom mikrostrukturom sa vremenom sferoidizacije. To se dovodi u vezu sa sferoidizovanim česticama karbida u ovom drugom, kao i uniformnom disperzijom karbida i visokotemperaturnog temperovanja martenzita u prvom. Tokom međukritičnog žarenja sferoidizovanih mikrostruktura, uočena je tendencija da se čestice martenzita dobiju kao izolovana ostrva. Ovo je rezultiralo lošijim odnosom čvrstoća-plastičnost u poređenju sa dvofaznim čelikom dobijenim međukritičnim žarenjem martenzita, što je negiralo korisnost sferoidizovanih mikrostruktura kao inicijalnih mikrostruktura za proizvodnju dvofaznog čelika.

Ključne reči: *Dvofazni čelik; Obrada sferoidizacijom; Mikrostruktura; Mehaničke osobine; Stopa naprezanja*